

Phase separation in a mixture of poly(ether sulphone) and poly(ethyl oxazoline): observation in real and reciprocal spaces

Hironobu Nakamura*, Junko Maruta, Takashi Ohnaga and Takashi Inoue†

Department of Organic and Polymeric Materials, Tokyo Institute of Technology,
Ookayama, Meguro-ku, Tokyo 152, Japan

(Received 5 January 1989; revised 12 April 1989; accepted 6 May 1989)

A mixture of poly(ether sulphone) and poly(ethyl oxazoline) was found to exhibit the lower critical solution temperature (*LCST*) type phase behaviour. The kinetics of phase separation after the temperature jump from the single-phase region to the two-phase region above the *LCST* was investigated in both real and reciprocal spaces, i.e. by light scattering, scanning electron microscopy (SEM), scanning transmission electron microscopy (STEM) and optical microscopy. The four different observations yielded an identical time variation of the periodic distance in the phase-separated structure. The early stage was well described within the framework of Cahn's linearized theory. In the late stage, the self-similarity in the structure was maintained throughout the coarsening process and the kinetics was described by the cluster dynamics by Binder and Stauffer. Unfortunately, direct observation of the concentration profile by elemental analysis by STEM was impossible.

(Keywords: poly(ether sulphone); poly(ethyl oxazoline); blend; spinodal decomposition; light scattering; scanning transmission electron microscopy; cluster dynamics; modulated structure)

INTRODUCTION

There have been many experimental studies on the demixing process of polymer-polymer mixtures¹⁻¹⁰. Some, on the initial stage of spinodal decomposition (SD), lead to the conclusion that the initial stage can be well described by the linearized theory proposed by Cahn¹¹ and modified by Cook¹². Others, on the late stage of SD, describe the reduced wavenumber of the dominant Fourier component of the concentration fluctuation Q_m and the reduced maximum scattered intensity I_m as functions of the reduced time τ ; ($Q_m \sim \tau^{-\alpha}$ and $I_m \sim \tau^\beta$) and compare experimental values of α and β with those predicted theoretically¹³⁻¹⁵. There also exists an argument in terms of the scaled structure function. Recently theoretical studies predict that α and β depend on the mode of coarsening¹⁶⁻¹⁹ and change with time of demixing^{20,21}. Anyhow, the discussion has been given mostly in reciprocal space. On the other hand, Cahn noted the importance of experimental studies in real space, i.e. direct observation of the continuous change in concentration fluctuation with demixing time¹¹.

We recently found *LCST* (lower critical solution temperature) type phase behaviour in a mixture of poly(ether sulphone) (PES) and poly(ethyl oxazoline) (PEOx). This is an interesting combination of dissimilar polymers for the study of SD, because both sulphur in PES and nitrogen in PEOx are expected to be sensitive species for elemental analysis by STEM (scanning transmission electron microscopy). For the particular combination, we intended to undertake direct observation of the concentration profile in the decomposed system and compare the results by other methods, such as light

scattering, SEM (scanning electron microscopy) and optical microscopy.

EXPERIMENTAL

The polymer specimens used in this study are poly(ether sulphone) (PES) (4100G, ICI, $M_w = 117\,000$) and poly(ethyl oxazoline) (PEOx) (XAS-10874.03, Dow Chemical Co. Ltd, $M_w = 200\,000$, $M_w/M_n = 2.5$). PES and PEOx were dissolved at 6 wt% of total polymer in dimethylformamide. The solution was cast onto a coverglass. After the solvent was evaporated at 60°C for 24 h, the cast film was further dried under vacuum (10^{-4} mmHg). The blend film thus prepared was clear and transparent. The blend film on the coverglass was inserted between a pair of steel blocks kept at a constant temperature and was annealed for 24 h in a nitrogen atmosphere. When the film became opaque and two-phase morphology was observed under an optical microscope, we judged that the blend was in the two-phase region in the phase diagram. When the film was still clear and phase separation could not be detected under a microscope, we judged that it was in the single-phase region. These annealing experiments were repeated at various isothermal settings. Thus we determined the phase diagram.

For the kinetics of demixing, particular attention was paid to the specimen with the critical composition 70/30 PES/PEOx (see *Figure 1*). Prior to the kinetic study, the solution-cast film was annealed at 200°C (in the single-phase region) for 30 min. The annealed specimen was inserted in a hot stage (Linkam TH600, Linkam Scientific Instruments Ltd) set at 240°C (in the two-phase region) and optical micrographs were taken at appropriate intervals.

The specimen annealed at 200°C was also inserted

* On leave from Sekisui Chemical Co. Ltd, Shimamoto, Osaka 618, Japan

† To whom correspondence should be addressed

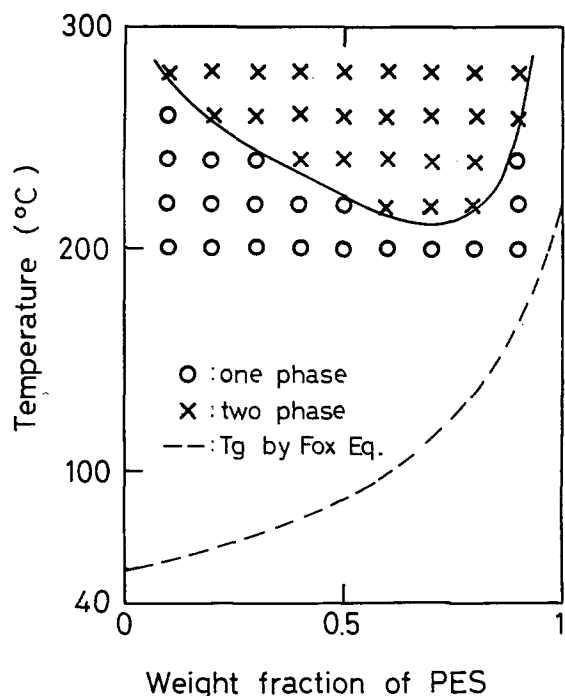


Figure 1 Phase diagram of PES/PEOx system

between a pair of steel blocks set at 240°C. After isothermal annealing, the specimen was quenched on another steel block set at 0°C. The quenched specimen was microtomed into ultrathin sections of $\sim 0.1 \mu\text{m}$ thickness and the frozen structure was observed under STEM (JEM-2000 FX, Nihon Denshi Co. Ltd). For SEM observation, the quenched specimen was fractured in liquid nitrogen and rinsed with water to extract PEOx.

In order to prevent oxidation during the light scattering measurement, the solution-cast film was covered with another coverglass in a hot press at 200°C for 30 min. The film specimen between the coverglasses was allowed to undergo a rapid temperature jump from 200°C to 240°C by dipping into a silicone-oil bath in a light scattering photometer. A He-Ne laser of 632.8 nm wavelength was applied vertically to the film specimen. The goniometer trace of the intensity of the scattered light was given at appropriate intervals during isothermal annealing.

RESULTS AND DISCUSSION

All of the solution-cast films with different compositions were optically clear. Even after annealing for 24 h at lower temperatures, the clarity was maintained and no indication of phase separation was seen under an optical microscope. This behaviour is indicated by open circles in Figure 1. By annealing at higher temperatures, some films became translucent or opaque and a modulated structure* with a periodic distance of a few micrometres was observed under a microscope (see Figure 6). This behaviour is indicated by crosses in Figure 1. On the basis of these observations, the cloud-point curve was drawn somewhat arbitrarily in Figure 1. It is a LCST type phase diagram with its critical point at 210°C and a composition of 70/30 PES/PEOx (weight ratio).

* A regular two-phase structure with unique periodicity and a high level of phase connectivity, which is supposed to be characteristic of the early stage of demixing by spinodal decomposition²²

By the linearized Cahn-Hilliard theory¹¹, the scattered intensity I is predicted to increase exponentially with time t :

$$I(q, t) = I(q, 0) \exp[2R(q)t] \quad (1)$$

where q is the wavenumber given by $(4\pi/\lambda)\sin(\theta/2)$, λ being the wavelength of light in the mixture and θ the scattering angle. The amplification factor $R(q)$ is given by:

$$R(q) = -Mq^2(\partial^2 f/\partial c^2 + 2\kappa q^2) \quad (2)$$

where f is the local free energy of mixing, c is the concentration, κ is the concentration-gradient energy coefficient and M is the mobility.

According to equation (1), a plot of $\ln I$ vs. t at a fixed q should yield a straight line of slope $2R(q)$. A linear relationship is realized for the initial stage of phase separation, as shown in Figure 2. It indicates that the initial stage can be described by the linearized theory. Linear results are also obtained at various q values.

Figure 3 shows a plot of $R(q)/q^2$ vs. q^2 . As expected from equation (2), the plot is a good straight line, indicating again that the initial stage can be described within the framework of the linearized theory. From the plot one can obtain such characteristic parameters as q_m , q_c and D describing the dynamics of phase separation: q_c is the critical (maximum) wavelength of fluctuations that can grow, q_m is the most probable wavenumber of fluctuation having the highest rate of growth. According to equation (2), q_c is given by the intercept on the q^2 axis, and q_m is calculated from the relation $q_m^2 = \frac{1}{2}q_c^2$.

The apparent diffusion coefficient D defined by $D = -M(\partial^2 f/\partial c^2)$ is given by the intercept on the vertical axis. The parameters thus obtained are $q_c = 18.7 \times 10^{-6} \text{ m}^{-1}$, $q_m = 13.2 \times 10^{-6} \text{ m}^{-1}$ and $D = 7.5 \times 10^{-17} \text{ m}^2 \text{ s}^{-1}$.

We examined the thermal noise effect pointed out by Cook¹². In order to escape from thermal noise, Sato and Han¹⁰ proposed recently the '1/3 power plot' based on

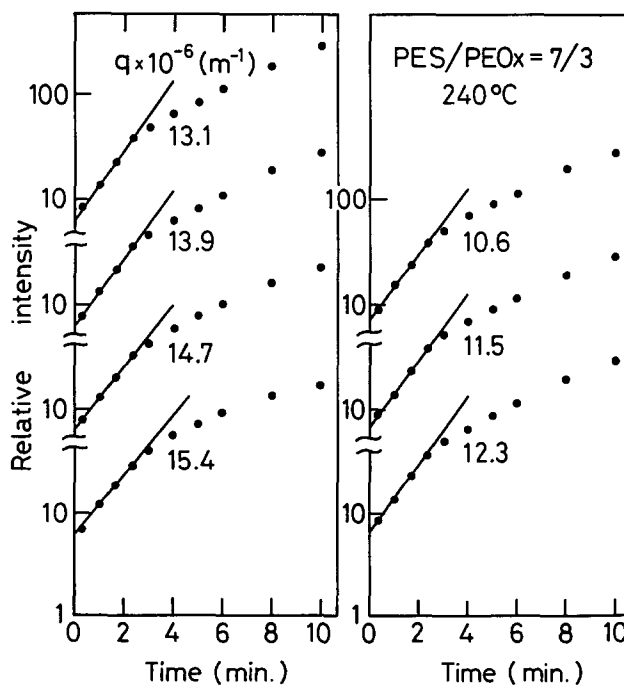


Figure 2 Change of the scattered intensity at various q values with time after the temperature jump to 240°C for 70/30 PES/PEOx

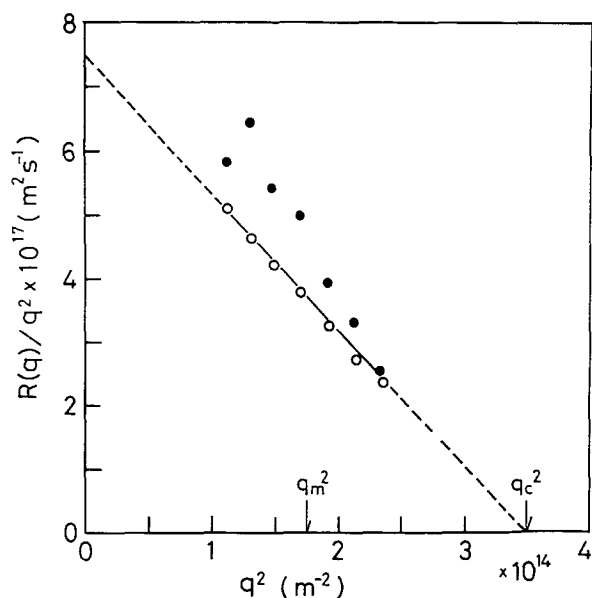


Figure 3 Plot of $R(q)/q^2$ vs. q^2 : open circles from $\ln I$ plot (Figure 2); full circles from the $1/3$ power plot

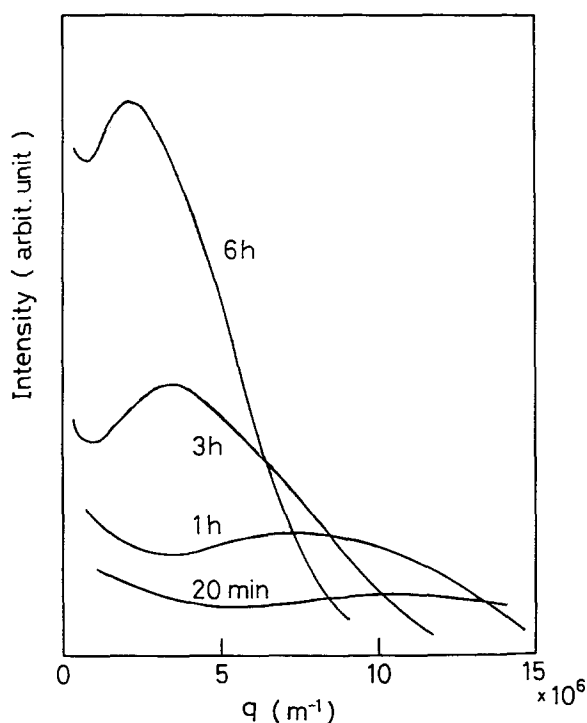


Figure 4 Change of light scattering profile with annealing. Numbers give the annealing time after temperature jump

an approximation (for $R(q)t < 1$):

$$\left(\frac{t}{I(q,t) - I_0}\right)^{1/3} = \frac{1}{[2(I_0 - I_\infty)R(q)]^{1/3}} \times \left(1 - \frac{1}{3}R(q)t + \frac{1}{81}[R(q)t]^3 + \dots\right) \quad (3)$$

where I_0 is $I(q, t=0)$ and I_∞ is $I(q, t=\infty)$. In the light of equation (3), we obtained $R(q)$ and then plotted $R(q)/q^2$ against q^2 . The results are indicated by full circles in Figure 3. The values of characteristic parameters q_c , q_m and D from this plot are almost equal to those from the $\ln I$ vs. t plot (open circles). This implies that the thermal noise effect is negligible for the phase separation at our deep quench.

At the late stage, the intensity of scattered light deviates from the exponential line as shown in Figure 2 and the scattering peak appears. Figure 4 shows the change of the scattered intensity profile $I(q)$ with demixing time at the late stage. The scattering peak is assumed to be due to the periodic structure developed by phase separation, i.e. the modulated structure. The peak position (q_m) shifts to smaller q with time. The variation of q_m will be shown in Figure 9. The results will be compared with those by different observations.

As expected from the results in Figure 4, the formation of modulated structure was observed under SEM. In Figure 5a, one can see the modulated structure that has been supposed to be characteristic of the result of spinodal decomposition. The periodic distance Λ_m of the modulated structure in Figure 5a is $\sim 0.45 \mu\text{m}$. This is almost equal to the correlation length ξ by the light scattering studies on the early stage (Figure 3), i.e. $\xi = 2\pi/q_m$. As shown in the four micrographs of Figure 5, the modulated structure grows self-similarly; in other words, the periodic and co-continuous characters are maintained throughout the coarsening process at the late stage even after 24 h. The time variation of Λ_m will also be plotted in Figure 9.

At the very late stage, the phase-separated structure can be observed by optical microscopy. The results are shown in Figure 6. Also from these results, one can estimate the time variation of Λ_m .

The development of modulated structure at the early stage was confirmed by STEM. Figure 7 is a TEM image by STEM, showing the identical structure to the SEM in Figure 5b.

Elemental analysis was performed under STEM. However, both nitrogen and sulphur were too insensitive to provide a direct estimation of concentration profile in the early-to-late stage. Sulphur mapping was barely possible. The white spots in Figure 8a mean that the intensity of the sulphur signal exceeds a threshold value. Note here that, in principle, the mapping yields a somewhat statistical image. If the S mapping is overlapped with the TEM image of Figure 7, one can see that the dark portion in Figure 7 is assigned to the PES-rich region. In order to demonstrate this more clearly, we drew full circles ($0.25 \mu\text{m}$ in diameter)* on each spot in Figure 8. This resulted in Figure 8b, showing the characteristic features of modulated structure.

All of the results thus obtained for the time evolution of Λ_m are summarized in Figure 9. These are plotted in the reduced variables, $\tau = (2\pi)^2 t D / \xi^2$ and $Q_m = q_m(t) \xi / 2\pi$ or $\xi / \Lambda_m(t)$, for comparison with the theoretical predictions in the early and late stages of spinodal decomposition. The plots fall onto a single curve. That is, the observations in both real and reciprocal spaces agree well. According to the recent studies by Snyder *et al.*⁴ and Hashimoto *et al.*⁸ on the polystyrene/poly(vinyl methyl ether) mixture, the master curve comprises the crossover of various processes, such as Cahn's linear regime¹¹, Binder and Stauffer's cluster regime¹⁹ and Siggia's interfacial instability regime¹⁶. In the present case, the late stage is nicely described by the cluster regime ($\alpha = \frac{1}{3}$). This seems to be reasonable, if one remembers

* Various values were applied for the diameter of the full circles. The diameter of $\sim 2.5 \mu\text{m}$ was found to be the best to embody the characteristics in the spot distribution

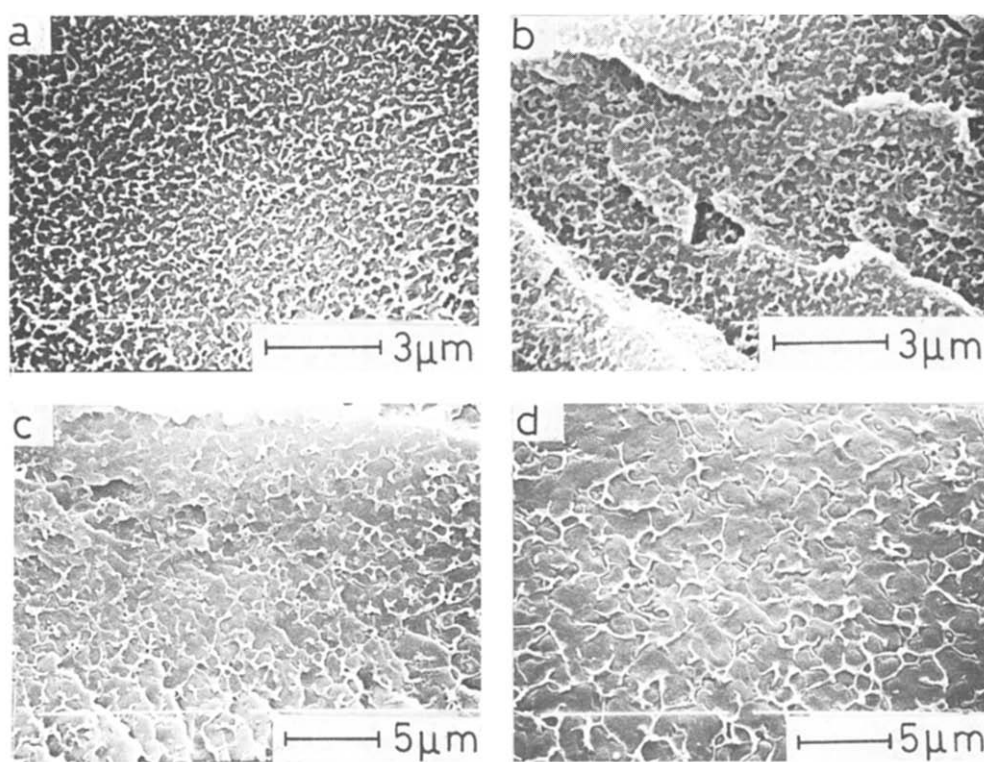


Figure 5 SEM micrographs of the 70/30 PES/PEOx mixtures after isothermal annealing at 240°C for (a) 6 min, (b) 20 min, (c) 1 h and (d) 6 h

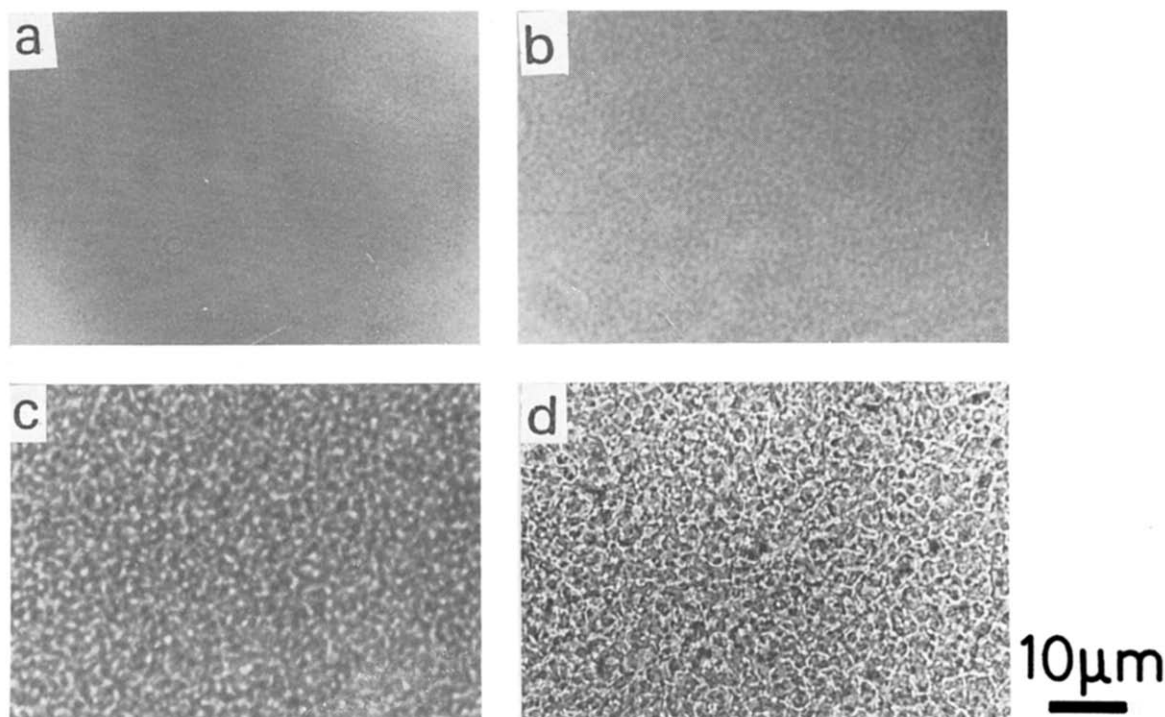


Figure 6 Optical micrographs of 70/30 PES/PEOx mixtures after isothermal annealing at 240°C for (a) 30 min, (b) 1 h, (c) 3 h and (d) 24 h

that the self-similarity in the structure development is maintained through the demixing process up to the very late stage.

CONCLUSIONS

The phase separation process of the critical mixture of PES and PEOx was investigated in both real and

reciprocal spaces. The early stage was well described within the framework of Cahn's linear theory. The development of modulated structure was visualized under SEM and STEM. The coarsening of modulated structure at late stage was described by the cluster dynamics of Binder and Stauffer. Unfortunately, direct observation of the concentration fluctuation was impossible even by the newest version of STEM.

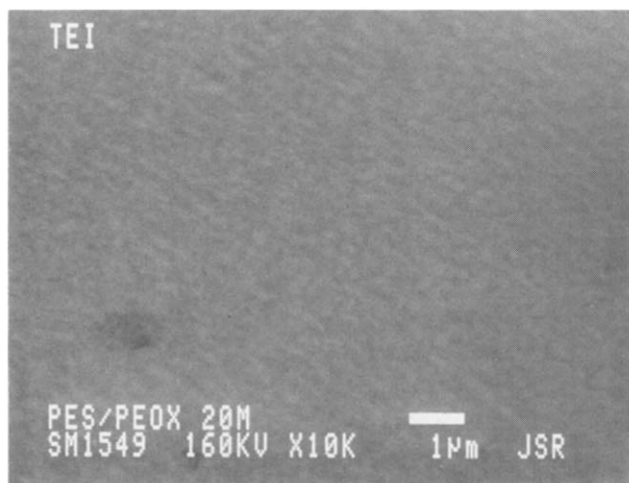


Figure 7 STEM image of the ultrathin section of 70/30 PES/PEOx mixture annealed isothermally at 240°C for 20 min

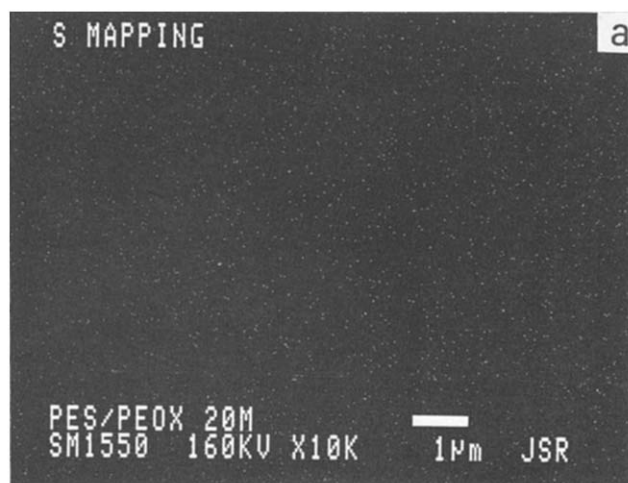


Figure 8 (a) S mapping of the specimen in Figure 7. (b) Modified S mapping: dots in (a) are widened to circles of 0.25 µm diameter

ACKNOWLEDGEMENT

We are deeply indebted to Mr Tetsuo Katsuta, Japan Synthetic Rubber Co. Ltd, for arranging for preparation of the scanning transmission electron micrographs.

REFERENCES

- 1 McMaster, L. P. *Adv. Chem. Ser.* 1975, **142**, 43
- 2 Nishi, T., Wang, T. T. and Kwei, T. K. *Macromolecules* 1975, **8**, 227
- 3 Nojima, S. and Nose, T. *Polym. J.* 1982, **14**, 907
- 4 Snyder, H. L. and Meakin, P. *J. Polym. Sci., Polym. Symp.* 1985, **73**, 217
- 5 Hashimoto, T., Kumaki, J. and Kawai, H. *Macromolecules* 1983, **16**, 641
- 6 Hill, R. G., Tomlins, P. E. and Higgins, J. S. *Macromolecules* 1985, **18**, 2555
- 7 Hashimoto, T., Itakura, M. and Hasegawa, H. *J. Chem. Phys.* 1985, **85**(10), 6118
- 8 Hashimoto, T., Itakura, M. and Shimadzu, N. *J. Chem. Phys.* 1986, **85**(11), 6773
- 9 Kyu, T. and Saldanha, J. M. *Macromolecules* 1988, **21**, 1021
- 10 Sato, T. and Han, C. C. *J. Chem. Phys.* 1988, **88**(3), 2057
- 11 Cahn, J. W. *J. Chem. Phys.* 1965, **42**, 93
- 12 Cook, H. E. *Acta Metall.* 1970, **18**, 297
- 13 de Gennes, P. G. *J. Chem. Phys.* 1983, **79**, 6387
- 14 Binder, K. *J. Chem. Phys.* 1983, **79**, 6387
- 15 Strobl, G. R. *Macromolecules* 1985, **18**, 558
- 16 Siggia, E. D. *Phys. Rev. (A)* 1979, **20**, 595
- 17 Lifshitz, I. M. and Slyozov, V. U. *J. Phys. Chem.* 1961, **19**, 35
- 18 Langer, J. S., Bar-on, M. and Miller, H. D. *Phys. Rev. (A)* 1975, **11**, 1417
- 19 Binder, K. and Stauffer, D. *Phys. Rev. (B)* 1977, **15**, 4425
- 20 Kawasaki, K. and Ohta, T. *Prog. Theor. Phys.* 1978, **59**, 362
- 21 Furukawa, H. *Phys. Lett. (A)* 1983, **98**, 28
- 22 Ougizawa, T., Inoue, T. and Kammer, H. W. *Macromolecules* 1985, **18**, 2089

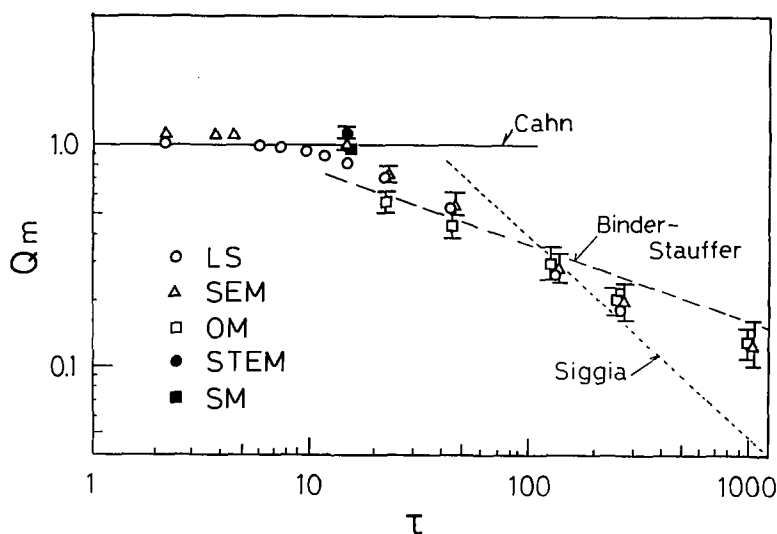


Figure 9 Time development of wavenumber q_m by different experimental techniques